Environmental Science & Technology

Article

pubs.acs.org/est

Duty Cycling Influences Current Generation in Multi-Anode Environmental Microbial Fuel Cells

Emily J. Gardel,[†] Mark E. Nielsen,[‡] Phillip T. Grisdela, Jr.,[§] and Peter R. Girguis*[,‡]

[†]School of Engineering and Applied Sciences, Harvard University, 29 Oxford Street Cambridge, Massachusetts 02138, United States

[‡]Department of Organismic and Evolutionary Biology, Harvard University, 16 Divinity Avenue, Cambridge, Massachusetts 02138, United States

[§]Department of Biology, Dartmouth College, 78 College Street, Hanover, New Hampshire 03755, United States

Supporting Information

ABSTRACT: Improving microbial fuel cell (MFC) performance continues to be the subject of research, yet the role of operating conditions, specifically duty cycling, on MFC performance has been modestly addressed. We present a series of studies in which we use a 15-anode environmental MFC to explore how duty cycling (variations in the time an anode is connected) influences cumulative charge, current, and microbial composition. The data reveal particular switching intervals that result in the greatest time-normalized current. When disconnection times are sufficiently short, there is a striking decrease in current due to an increase in the overall electrode reaction resistance. This was observed over a number of whole cell potentials. Based on these results, we posit that replenishment of depleted electron donors within the biofilm and surrounding diffusion layer is necessary for maximum charge transfer, and that proton flux may be not limiting in the highly buffered aqueous phases that are common among environmental MFCs. Surprisingly, microbial diversity analyses found no discernible difference in gross community composition among duty cycling treatments, suggesting that duty cycling itself has little or no effect. Such duty cycling experiments are valuable in determining which factors govern performance of bioelectrochemical systems and might also be used to optimize field-deployed systems.

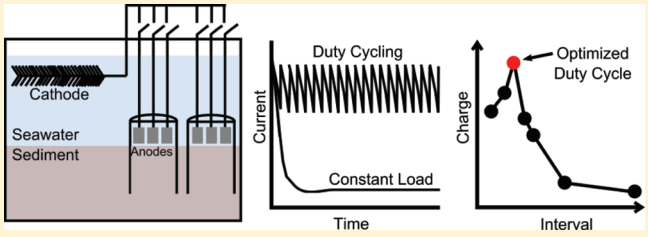

INTRODUCTION

Microbial fuel cells (MFCs) harness the catabolic activity of microorganisms to convert chemical energy into electrical energy.[1,2] Electroactive microorganisms facilitate the exchange of electrons to and from solid-phase electron acceptors or donors through diverse physiological mechanisms that we will broadly refer to as extracellular electron transfer (EET).[2−9] MFCs operated in nature, or in comparable, industrial conditions such as sewage treatment plants, are referred to herein as environmental microbial fuel cells (eMFCs), and typically host a diversity of microbes on the anode that may be directly or indirectly involved in EET.[2,10,11]

MFCs have been the subject of much research in the past decade,[12−14] largely driven by the possibility to produce substantial amounts of carbon-neutral energy from organic matter, including wastewater, as well as the promise of catalyzing the efficiency of industrial processes that rely on microbial catabolism.[15−19] There have been a number of suitable implementations of eMFCs for small-scale power generation, such as unattended power supplies for distributed sensors,[20,21] though power from eMFCs is often below the amount required for most conventional external devices. For example, numerous eMFC studies report power densities ranging from 20 to 1500 $mW{\cdot}m^{-2}$ normalized to anode area,[22−27] with systems using defined media producing more power in general.[10] Moreover, additional losses are often incurred when scaling up MFCs, which result from design and technological constraints.[28−30] To increase the efficacy of MFCs, in particular eMFCs, in power production, recent studies have endeavored to increase power through the use of particular microbial phylotypes,[31−34] varying electron donors,[35−37] electrode materials,[38,39] the addition of electrochemically active compounds[6,8,40,41] to facilitate electron transfer between the microbes and the electrode, and optimizing system function and architecture, through various buffers[27,42] and use of selective membranes.[43]

Whereas the influence of design factors on MFC performance has been extensively studied, the extent to which duty cycling affects MFC performance has been of interest only recently and is further addressed in this study. Recent duty cycling experiments performed by connecting and disconnecting to an external resistor in an MFC concluded that shorter cycles lead to optimal power production.[44] Previously, a capacitor has been used in the external circuit to accumulate charge and release bursts of current discharged either through an external resistor[45] or channeled back to the anode as in a microbial electrolysis cell.[46] In these studies, the circuit design

Received: December 22, 2011
Revised: April 11, 2012
Accepted: April 12, 2012
Published: April 12, 2012

resulted in a variable anode potential that can influence microbial colonization and activity and, potentially, power production.[47,48]

Fundamental to all MFCs are the limitations imposed by the diffusion of substrates and products into and out of microbial cells and, in some cases, into and out of the microbial biofilm. Recent laboratory studies using pure or defined cultures reveal that substrate diffusion in the biofilm[49] and proton diffusion away from the anode[42] limit current generation. These studies highlight important factors that influence the electrode reaction kinetics associated with MFC performance: donor-substrate availability and utilization, electron transfer to the anode, and proton diffusion away from the anode.

It is equally important to consider how these and other factor(s) might govern power production in eMFCs. For example, the extent to which the surrounding geochemical environment or microbial community composition influences bulk transport, alleviates diffusion limitation, and, ultimately, affects power production is unknown. To this end, we conducted a series of experiments in which we operated a multiple anode eMFC (specifically a chambered MFC placed atop marine sediments) to interrogate how three key factors—substrate and endproduct diffusion into and out of the biofilm, microbial community composition, and geochemical conditions—influence power production. Through cycling continuity between anode and cathode at varying frequencies, geochemical analyses, and molecular microbial phylogenetic analyses, we characterized the relationship between current production and cycling frequency, seawater geochemical composition and pH, biofilm thickness, and microbial community composition. We held the potential constant with a programmable load during these experiments to eliminate variable potential as a confounding factor. These data suggest that replenishment of depleted chemical species within the biofilm and surrounding diffusion layer is likely what governs maximum charge transfer in these eMFCs. It is also worth noting that duty cycling had no discernible effect on microbial community composition, suggesting that gross community composition is unaltered by duty cycling in these experiments. In brief, these data collectively underscore the importance of considering a variety of operational, geochemical, and microbial factors when characterizing or optimizing MFC performance.

EXPERIMENTAL METHODS

System Design and Operation. We built a multianode chambered benthic MFC (Figure S1) in an aquarium (40 cm deep × 60 cm long × 30 cm high) filled with saltmarsh sediment recovered from Winthrop Harbor, MA to a height of approximately 24 cm. The remainder of the tank was filled with natural aerated seawater. The multianode MFC consisted of 15 graphite anodes, housed in sets of three, in five independent semi-enclosed acrylic chambers. Anodes were fabricated from cylindrical graphite rods (1.25 cm diameter × 1.25 cm high). Each chamber was 7 cm in diameter and 15 cm high, and were pushed approximately 10 cm into the sediment. The top of each chamber was fitted with a gastight septum to enable fluid sampling. All the anodes were connected to a programmable relay board (model 34903A; Agilent Inc.) that enabled the independent connection of each anode to a custom-built programmable load (North-West Metasystems, Inc.).[26] The circuit effectively adjusts the external resistance to maintain a user-defined whole-cell potential (in our case 0.5 V), so long as actual whole-cell potential is not below the user-defined set point. To eliminate variations in cathode performance, a single 1-m long graphite brush was used as the cathode for all experiments. The cathode was placed in the overlying, air-sparged seawater (S = 30 ppt, T = 10 °C) overlying the sediment in the aquarium. Our measurements of constant cathode potential during all duty-cycling treatments indicate that our system was not cathode-limiting. An Ag/AgCl electrode (MI-402; Microelectrodes, Inc.) was used as a reference electrode in the overlying water. Electrode potentials and current were measured using a digital multimeter (34970A; Agilent Inc.) with 6 1/2 digits of resolution, 0.004% direct current (DC) voltage, and isolated from the earth-referenced circuitry and computer interface. A 20-channel multiplexer and 2 current channels module (34901A; Agilent Inc.) with a 60 channel·s^{-1} scan speed and 120 channel·s^{-1} open/close speed was used to input electrode potential and current for measurement.

The multimeter and relay bank were controlled through a custom-designed LabVIEW interface with the capability to execute a number of different experiments: (1) cycling among all 15 anodes with a set switching interval (1.5 s data acquisition), (2) cycling a single anode through variable ON and OFF times (600 ms data acquisition), and (3) maintenance of the anodes at a constant state (i.e., always ON or always OFF). Cycling among all 15 anodes sequentially allowed current to be drawn from one anode at a time, and single experiments were conducted at different anode switching intervals (3 s, 7.5 s, 15 s, 30 s, 60 s). The "ON" time was the switching interval, i, and the "OFF" time was the total amount of time it took to cycle back to the same anode, $(n - 1) \times i$ for the general case of n anodes and $14 \times i$ for our case of 15 anodes. Later, a single electrode was used for select duty cycling experiments (where each condition was performed once), wherein each set of cycling conditions was followed by a period at open circuit until anode potential was within 1.5% of the original open circuit value (to remove any experimental carryover effects). Using a single anode in this manner enabled the ON and OFF times to be investigated independently to measure total cumulative current passed by the anode. Selection of the cycling conditions, the ON and OFF times, between consecutive experiments was varied to reduce any bias in the system. In these experiments, the total sum of ON times was normalized to one hour in order to compare how the OFF time interval influenced total cumulative charge. Maintaining constant continuity with a steady whole cell potential was used to study pH changes within the pore water inside the core tube.

pH Measurements. pH was monitored inside one chamber for nine consecutive days, during which the three electrodes in the chamber were kept in the ON state. Fluid samples (2 mL) were collected from within the chamber through the septa in the lid at regular intervals, decanted into a 2-mL centrifuge tube immersed in a 10 °C cold bath, and measured with a needle pH electrode (MI-407; Microelectrodes, Inc.) with an Ag/AgCl electrode (MI-402; Microelectrodes, Inc.) as reference using a pH meter (AR20 Accumet; Fisher Scientific). All pH samples and measurements were conducted in duplicate.

Dissolved Sulfide Measurements. Anode chamber fluid was collected through the septa, and dissolved sulfide was measured with a spectrophotometer sulfide kit scaled down to handle sample volumes of 1 mL (LaMotte, Inc.). Absorbance was measured with spectrophotometer (DU-650; Beckman-Coulter) and was compared to a standard curve of known concentration sodium sulfide samples prepared anaerobically.

Both chamber fluid and a 10*x* dilution with Milli-Q water were measured for an accurate reading on the standardization curve.

Assessing Changes in Anode Biofilm Diversity Across Treatments. Microbial diversity was assessed by examining the community diversity of the electrogenic biofilm growing on four representative anodes maintained at four different duty cycles: (a) always ON, (b) 1.8 s ON and 0.6 s OFF, (c) 1.8 s ON and 41.4 s OFF, and (d) always OFF. After operating at these conditions for four months, electrodes were removed from the system and scraped with a sterile razor blade. Shavings were scraped into sterile cryovials. In addition, sediments underlying the electrodes were sampled using syringes with the tips removed, and biofilm from inside each chamber were sampled using sterile wipes (Kimberley Clark, Inc.). All samples were flash frozen in liquid nitrogen and then kept at −80 °C until further processing.

DNA was extracted using a PowerSoil DNA Isolation Kit (Mo-Bio, Inc.) following the manufacturer's protocol, with an additional cell lysis protocol consisting of heating to 85 °C and bead beating (FastPrep-24, MP Bio, Inc.) for 60 s at 6.5 m/s after the initial extraction. DNA extractions were quantified using a fluorometric assay (Qubit; Invitrogen, Inc.), and ranged from 25 to 300 ng of DNA·cm^{-2} of electrode, with the anode in the always OFF state having the least concentration.

16S rRNA genes were amplified by PCR with 28F (5′-GAGTTTGATYMTGGCTC) and 519R (5′-GTAT-TACCGCGGCTGGCTG) primers as previously described,[50] and amplicons were sequenced via 454 Titanium pyrosequencing.[51] Sequence sff files were analyzed with Qiime version 1.3.0,[52] OTUs were picked with the optimal flag passed in UCLUST with a 0.97 similarity threshold and a representative set was selected based on the most abundant sequence and aligned with PyNAST using the UCLUST pairwise alignment method with a 0.75 minimum percent sequence identity to closest BLAST hit to include sequence in alignment. ChimeraSlayer was used to identify chimeric sequences before the OTUs were assigned taxonomy with the RDP database at a minimum confidence level of 80%.

Sequence sff files are available through the National Center for Biotechnology Information Sequence Read Archive (NCBI SRA) database under submission identification SRA049469.

Scanning Electron Microscopy (SEM) Sample Preparation and Imaging. Anode subsamples for SEM imaging were collected at the same time as those for DNA extraction. A section of the anode was removed using a sterile cutter and immediately placed in 2 mL of sterile 5% glutaraldehyde in phosphate buffered saline (PBS), in a sterile 2-mL centrifuge tube and held at 4 °C for 24 h. The samples were subject to ethanol dehydration by placing the sample in 10%, 25%, 50%, 75%, and 100% ethanol (200 proof) PBS solutions for 5 min each. The 100% ethanol solution was changed three times and the sample was left in ethanol for critical point drying (Autosamdri 815 A; Tousimis, Inc.) with a 15-min purge time. The samples were adhered to SEM posts with carbon tape and coated with platinum/palladium (208HR Sputter Coater) at 40 mA current for 100 s and then imaged with a SEM at 10 kV (JEOL, Inc.).

Confocal Microscopy Sample Preparation, Imaging, and Analysis. Anode sections were sampled as above, and placed into a sterile 4% paraformaldehyde in PBS solution in a 2-mL centrifuge tube and refrigerated at 4 °C for 12 h. Samples were placed in 100% PBS and kept at 4 °C. Prior to imaging, each sample was placed with sterile tweezers in 500 μL of PBS and 0.15 μL of SYBR Green I (Invitrogen), wrapped in foil, and kept at room temperature for at least 15 min. Samples were then placed in a PBS-filled glass-bottom dish (MatTek Corp.), with the side to be imaged against the coverslip, and imaged with a Zeiss 700 inverted confocal microscope using the 488-nm laser and Zeiss filter set 38. For calculating biofilm thickness measurements, confocal stacks were imaged at 20×, 40×, and 63× magnifications with typical *z* distances between each slice being 1.7, 0.4, and 0.3 μm, respectively. Different magnifications were used to reduce any bias due to slice thicknesses. In total, eight confocal stacks were acquired for always ON, short OFF, and long OFF samples. Due to the inherent heterogeneity of both the graphite surface and the biofilm thickness, each image was analyzed with an ImageJ program that subdivided each stack into a 10 × 10 grid and calculated the local biofilm thickness based on signal intensity for each sub region. The average biofilm thickness is from the values for sub regions among all images for a given sample.

RESULTS AND DISCUSSION

Defining Mass Transfer Limitation in MFCs. In a MFC, the magnitude of the steady-state current is usually limited by one reaction, typically called the rate-determining step. The more facile reactions are held back from their maximum rates by the slowness with which the rate-determining step disposes of their products or creates their reactants. The electron exchange reaction at the electrodes can be represented by a resistance term (R) composed of a series of resistances: mass transfer between the bulk solution and near the electrode surface, chemical reactions that occur within this region close to the electrode, and surface reactions including adsorption, or desorption, and electron transfer at the electrode (eq 1). A fast reaction step is characterized by a small resistance, while a slow step is represented by a high resistance.

$$R = R_{\text{mass-tansfer}} + R_{\substack{\text{chemical}\\\text{reactions}}} + R_{\substack{\text{surface}\\\text{reactions}}} + R_{\text{electron-transfer}} \quad (1)$$

Generally, eMFC systems that are operated continuously become mass-transfer limited. Previous studies have shown that the power density of an eMFC is increased 4-fold by mixing the fluids in the anode chamber.[22] Similarly, the mass-transfer resistance can be reduced by disconnecting the anode to enable substrate depletion to dissipate through diffusion. Cycling a series of anodes then is expected to lower the overall electrode reaction resistance and increase the current produced, when compared to a single anode under constant load.

Effect of Anode Switching on Cumulative Charge. In our experiments we tested seven different anode cycling intervals, in which the "ON" period is defined as the length of time that a single anode was connected to a cathode. Using a metric of cumulative charge per day, we observed an optimal cycling interval of 15 s ON per anode (Figure 1a), which yielded 17 coulombs per day. This optimal cycling interval is, to a degree, a function of the number of anodes in our system, which in this case determined the extent of OFF time. Notably, the shorter time intervals of 3 and 7.5 s yielded less charge than the optimal 15 s, most likely due to a shortened OFF time, implying that there is a benefit to allowing the anodes to reside at open circuit. In addition to the OFF time interval dependence, the number of ON/OFF cycles varies with switching interval. Single anode experiments were conducted to remove the interdependence of the ON and OFF times in

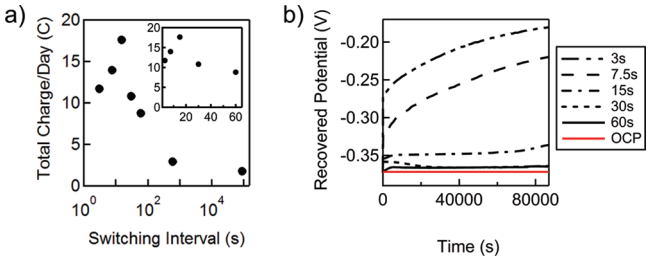

Figure 1. (a) Total charge cumulated over a 24-h period from sequentially switching among 15 anodes at a specified interval (a single anode is always connected to the cathode). The inset presents the same data plotted on a linear *x*-axis to resolve the shorter switching intervals. (b) Recovered potential of a single anode measured at the end of each OFF time interval as a function of time for different switching intervals. Recovered potential is the minimum potential reached by the anode during one duty cycle. The open circuit potential (OCP) prior to the experiment is plotted in red to demonstrate the deviation of the recovered potential. OFF intervals of less than 15 s demonstrate an inability of the anode to recover during repeated duty cycles.

the 15 anode experiments. With a single anode, different combinations of ON and OFF times were selected and duty cycling continued until the total amount of ON time equaled 1 h. These single-anode experiments demonstrate that select ratios of ON/OFF times yielded greater total charge normalized to 1 h of total ON time (Figure 2).

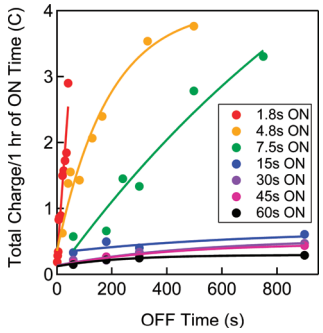

Figure 2. Cumulative charge per 1 h of combined ON time as a function of the OFF time interval in the duty cycle experiment. Each point corresponds to a single experiment at the specified ON and OFF times. The curves are exponential fits, $Y = A + Be^{-Cx}$, for illustrative purposes only.

Examining the current profile of an ON/OFF cycle in a single-anode experiment (Figure S2) demonstrates how a shorter switching interval leads to more cumulated charge due to less time spent in the current profile's plateau, where current is modest. All current profiles (both single and multianode experiments) exhibited $\sim t^{1/2}$ decay rate that is typical when a voltage step is applied to an electrode.[53] This most likely results from the expanding diffusion layer, $\partial_O(t)$, surrounding the electrode where the oxidizing species are depleted. The thickness of the diffusion layer depends on the time after the voltage step (t) and the diffusion coefficient of the oxidizing species (D_O), grows with $\sim t^{1/2}$ (eq 2) and reaches a maximum when the concentration gradient through the diffusion layer reaches a steady-state.[53]

$$\partial_O(t) = 2\sqrt{D_O t} \tag{2}$$

The time shortly after connection when the diffusion layer is thin, produces maximal current because the electrode is surrounded by a high concentration of electron donors, be they reduced chemical species that are abiotically oxidized by the anode or microbial cells replete with charge from their metabolic substrates.[26,49]

These experiments demonstrate the value of allowing the system to spend time in open circuit if maximal current is a key characteristic being optimized. At switching intervals shorter than 15 s, the multianode experiments yielded less charge, decreasing the overall benefit of a shorter ON time. Indeed, previous experiments using pure cultures of *S. oneidensis* MR-1[54] and *Geobacter sulferreducens*[55] observe similar current profiles (a transient peak with $\sim t^{1/2}$ decay) following circuit connection with peaks that increase in magnitude with longer time spent in open circuit. The authors attribute the increased current to the biofilm's ability to store charge that accumulated during the disconnection time. The transient current peaks observed in our experiments are consistent with the discharging of charge stored in the biofilm, but our data do not provide the resolution needed to definitively attribute our results to this phenomenon.

Recovery of Anode Potential during Cycling. To further elucidate the effect of the OFF time to the overall system performance, we examined the anode potential profiles of the different switching intervals in the 15 anode experiments, and observed that anode potential prior to the next ON time—which we refer to as recovered potential—is closer to the original open circuit potential at longer time intervals (Figure 1b). During these experiments, 15 s is the shortest switching interval where the anode potential nearly fully recovers to open circuit potential, suggesting that for any given system a specific combination of ON time and OFF time maximizes anode potential recovery while increasing total cumulative charge. We parameterized this anode recovery by calculating the anode recovery percentage, which is defined as the ratio of the difference between the anode recovered potential, V_R, (Figure S2a) and the anode closed circuit potential, V_{ON}, and the difference between original open circuit potential, V_{OCP}, and anode closed circuit potential, V_{ON} (eq 3).

$$\text{AR}\% = \frac{|V_R - V_{ON}|}{|V_{OCP} - V_{ON}|} \times 100 \tag{3}$$

If the anode fully recovers during the OFF time, then this anode recovery percentage is 100%. For each of the single anode experiments, the average anode recovery percentage is compared to the average height of the current peaks that occur immediately after connection of the anode to the cathode. The OFF time influences the anode potential and, when sufficient in length, allows the anode to recover to open circuit potential, which increases current when the anode is in continuity. The data reveal, not surprisingly, that the longest OFF time yields the greatest recovery (Figure 3). However, at OFF times less than 10 s, anode recovery is never better than 20% and the average height of the current peaks drastically decreases by half. Thus, if optimizing for current, aggressive duty cycling may not be any more beneficial than leaving the electrode in continuous continuity.

To better understand the basis of these findings, we used a resistor−capacitor in series as an equivalent circuit, although typical equivalent circuits used to represent microbial fuel cells contain more components when more analysis is desired.[56,57]

dx.doi.org/10.1021/es204622m | Environ. Sci. Technol. 2012, 46, 5222−5229

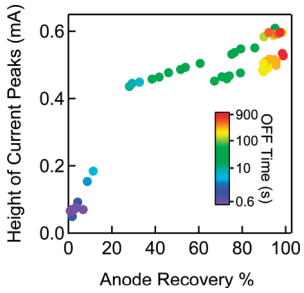

Figure 3. Average height of the current peaks plotted versus average anode recovery percentage. Each point represents a single experiment. The markers are color coded to the OFF time used in that experiment.

An ideal voltage step experiment, where faradaic reactions occur fast and charge transfer resistance is negligible, can be represented by a bulk capacitance (C) and a resistance (R). It is the same as in an RC circuit (eq 4) where applying a potential step (V) has a current (i) and a response over time (t). At $t = 0$, the height of the current peak is equivalent to V/R. In these experiments, the anode potential is the same while connected, therefore any change in the current peak height indicates a change in the overall resistance in the electrode reactions; a lower current means the reaction rate is limited.

$$i = \frac{V}{R} e^{-t/RC} \tag{4}$$

When the height of successive current peaks and anode recovery percentage is followed throughout the course of the experiments, those with OFF times of less than 7 s show a sudden drop in current peak height around 15% anode recovery (Figure S3). Recall that each experiment starts at 100% recovery because the system rested in open circuit and proceeds to lower percentage values as the experiment progresses. For the experiments with the longest OFF time, 498 s, the recovery percentage never drops below 80%. These findings indicate that there is a threshold anode recovery percentage below which the current passed during ON time decreases substantially due to an increased resistance of the electrode reactions.

To determine whether the anode potential is important for recovery (represented by current peak height), we conducted an additional series of single anode experiments where the switching conditions were the same (1.8 s ON and 0.6 s OFF) but the whole cell potentials were 0.25 V, 0.5 V, 0.6 V, and 0.7 V (Figure S4). These data reveal that the whole cell potential modestly influences the height of the current peaks and does not alter the minimum percentage of anode potential recovery obtained during the course of the experiment, implying that OFF time is important for reaching anode recovery.

Biofilm Constraints on Transport. Because our data suggest that time is the critical parameter, it is apparent that diffusion of metabolites, including protons, substrates, or both, within the biofilm, is the major factor that governs current production. To that end, we used the 1-D diffusion equation (eq 2) to calculate a length scale associated with this time using typical diffusion coefficients of substrates through a biofilm. With these values, we empirically estimated a length of ~100−200 μm for substrates larger than protons, which have a range of ~400−600 μm (Table S1). As mentioned, the relationship between time and diffusion coefficient calculates the diffusion layer boundary surrounding the anode and, in our case, this layer is comprised of both biofilm and surrounding liquid. Imaging with SEM (Figure 4a and b) and confocal microscopy (Figure 4c) demonstrate highly comparable biomass on all

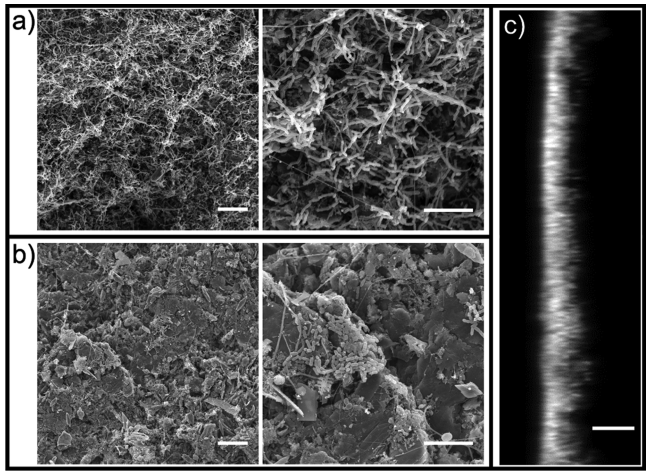

Figure 4. (a, b) SEM images of (a) an anode that was continuously connected to a cathode, and (b) an anode that was disconnected. Each pair of images is of the same sample at two different magnifications: 600× (left) with a corresponding 20 μm scale bar and 2000× (right) with a 10 μm scale bar. (c) Confocal microscopy z-profile of an always ON anode (30 μm scale bar). Confocal stacks of the two duty-cycled anodes (with short and long OFF times) have similar thicknesses.

active (cycled) anodes, demonstrating that interruption time does not influence overall microbial mass. Confocal microscopy shows that all active anodes have a similar thickness of 30 ± 10 μm (Figure 4c). Our calculated length is larger than the thickness of the biofilm and, therefore, includes a diffusion layer beyond the biofilm surrounding the anode. If the maximum diffusion layer is on the same order of magnitude as a previous study, which calculated a maximum diffusion layer distance of ~50 μm,[49] then 5−10 s corresponds to the amount of time it takes for species to sufficiently pass through both the maximum diffusion layer and the biofilm surrounding the anode. The correspondence between time and length scales in our experiment implies that our observed increase in electrode reaction resistance may be attributable to the diffusion layer, namely when it is at its maximum.

Through this analysis we cannot infer which metabolite in particular is the limiting factor. However, it is known that protons have a very high diffusion coefficient and we sought to determine if this was an important factor in our system by monitoring pH in the anode chamber. Previous experiments have found that diffusion of protons from the anode biofilm to the cathode is the rate-limiting step in current production.[42] Herein, by maintaining all three anodes under continuous load (which would result in the greatest excursion in pH) resulted in a modest change in chamber seawater pH from 7.1 to 6.9 over a period of 9 days (Figure S6). We determined that seawater with 1500 μM sulfide (comparable to our conditions of 1300−1700 μM) typically has a total alkalinity of 3.1 meq·L^{-1},[58] which in combination with sediment alkalinity provides highly effective buffering of protons in solution. As previously observed, an increase in the buffering capacity of the medium in a laboratory MFC increases current production.[42] Conversely, a study of *Geobacter sulferreducens* biofilms on MFC anodes found a striking reduction in pH within the biofilm.[59] Although we are unable to determine the extent to which the biofilm

dx.doi.org/10.1021/es204622m | *Environ. Sci. Technol.* 2012, 46, 5222−5229

accumulates protons in these experiments, we have determined that the modest change in seawater pH decreased seawater alkalinity by less than 20%,[60] and the remaining buffering capacity of both the seawater and the sediments make it highly likely that proton diffusion out of the biofilm into the well-buffered media—and conversely the diffusion of buffering constituents into the biofilm—was both rapid and effective at mitigating proton accumulation.

Microbial Community Composition of Anode Biofilms. Analyses of the 16S rRNA gene sequences revealed that microbial community composition was, at a coarse level, highly similar among all active anodes (Figure 5). These communities

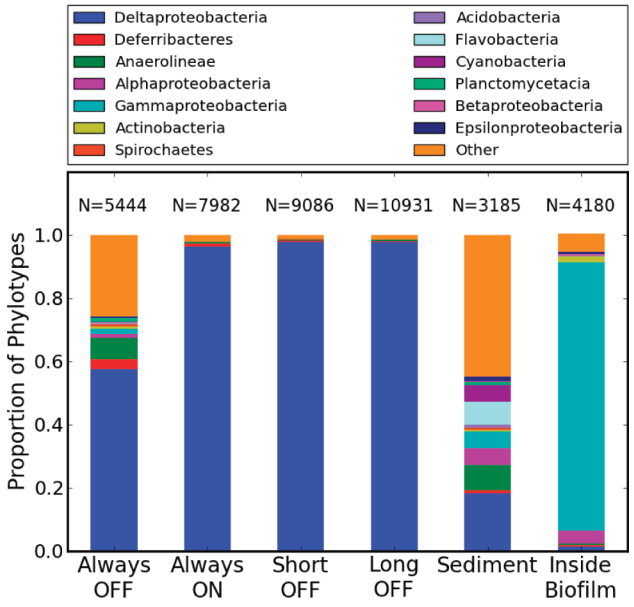

Figure 5. Class level representation in the one inactive anode (always OFF), the three active anodes (always ON, short OFF, and long OFF), sediment, and biofilm inside the core tube. *N* = the number of sequences represented in each bar. See Experimental Methods for details.

were dominated by Proteobacteria with at least 98% representation, regardless of duty cycle. In contrast, the control (open circuit) anode hosted 70% Proteobacteria. In all three active anodes, we observed a significant enrichment of δ-proteobacteria, representing ~98% of all the 16S rRNA gene sequences recovered from active anodes (Figure 5); 66% of the sequences on the control electrode (always OFF) and 21% of the sequences in the sediment were assigned to the δ-proteobacteria. Sequences recovered from a nonelectroactive biofilm accumulated on the inside of the chamber were enriched with 85% γ-proteobacteria and 4% α-proteobacteria. For the three active anodes, ribotypes allied to the genus *Desulfobulbus* were dominant making up 96–97% of all recovered gene sequences, but only 35%, 1%, and 0.4% of the sequences from the control anode, sediment, and inside biofilm, respectively (Figure S5). Although these high-throughput sequence representations are not quantitative, the clear dominance of these ribotypes strongly suggest they are the dominant members of the community and—after establishment of the community—are likely the dominant contributors to power production.

Implications and Applications. Collectively, these data provide a comprehensive empirical assessment of power production as a function of duty cycling frequency and further our understanding about which factor(s) influence and govern power density in electroactive biofilms. Previous models have suggested that proton diffusion limits power production, but in the highly buffered conditions of this experiment and resolution of our measurements, this does not appear to apply. Rather, replenishment of metabolic substrates via diffusion into the biofilm appears to govern power density and varying the ON–OFF state enables these substrates to diffuse into these substantial biofilms. In general, the evaluation of power output curves in microbial fuel cells should take into account that current after disconnection events can be considerably higher than current produced under steady-state conditions. We do recognize that we are unable to comment on the specific rate of diffusion or acquisition of metabolites into the cells, or the metabolic rate of sulfide oxidation, or electron shuttling via outer membrane cytochromes or redox active shuttles, and future experiments might aim to constrain these factors and their role in eMFC performance.

Although it is apparent that the OFF time does not produce current, and as such when integrated over time that duty cycling may yield less total power, there is operational value in duty cycling. First, this is relevant to applications where voltage is boosted to harness energy or operate instrumentation, as the higher input voltage results in greater power conversion efficiency. Additionally, this may be relevant to the field of bioelectrosynthesis wherein electrodes provide electrons as reducing equivalents for the production of organic molecules, e.g., biofuels or high-value pharmaceuticals. The ability of a microorganism to utilize charge from a solid-phase electron donor is influenced by the potential of that electrode, and the availability of substrates in the surrounding media. With the recent focus on electrosynthesis,[66] duty-cycling to optimize for these factors might well yield higher net product. It is equally possible that in these systems the organisms do not require a constant electrode potential to produce the desired output, and switching anode connection could significantly reduce the operating costs of running the system. As in these experiments, there might be minimum anode potential beyond which the current significantly decreases. It is important to fully investigate the deployed system to make sure it is operating above this minimum.

■ ASSOCIATED CONTENT

Ⓢ Supporting Information

System schematic; profiles of current and potential from one duty cycle; data of current peak height versus anode recovery percentage; data with varying whole cell potential; family level microbial community representation; diffusion coefficients and calculated distances of relevant metabolites.This material is available free of charge via the Internet at http://pubs.acs.org.

■ AUTHOR INFORMATION

Corresponding Author

*Phone: 617-496-8328; fax: 617-496-8328; e-mail: pgirguis@oeb.harvard.edu.

Notes

The authors declare no competing financial interest.

■ ACKNOWLEDGMENTS

This material is based upon work supported by the National Science Foundation under Grants MCB-0702504 and OCE-

0732369. The information, data, or work presented herein was funded in part by the Advanced Research Projects Agency – Energy (ARPA-E), U.S. Department of Energy, under Award DE-AR 0000079. This research was also supported in part by the Department of Energy Office of Science Graduate Fellowship Program (DOE SCGF), made possible in part by the American Recovery and Reinvestment Act of 2009, administered by ORISE-ORAU under contract DE-AC05-06OR23100. This work was performed in part at the Harvard Center for Nanoscale Systems (CNS), a member of the National Nanotechnology Infrastructure Network (NNIN), which is supported by the National Science Foundation under NSF award ECS-0335765 and the Harvard Center for Biological Imaging. The computational analysis of the 16S gene sequences in this paper was run on the Odyssey cluster supported by the FAS Science Division Research Computing Group at Harvard University. We thank J. Aizenberg for use of the scanning electron microscope.

REFERENCES

(1) Logan, B. E.; Hamelers, B.; Rozendal, R.; Schroder, U.; Keller, J.; Freguia, S.; Aelterman, P.; Verstraete, W.; Rabaey, K. Microbial fuel cells: Methodology and technology. *Environ. Sci. Technol.* **2006**, *40*, 5181–5192.

(2) Lovley, D. R. Bug juice: Harvesting electricity with microorganisms. *Nat. Rev. Microbiol.* **2006**, *4*, 497–508.

(3) Hernandez, M. E.; Newman, D. K. Extracellular electron transfer. *Cell. Mol. Life Sci.* **2001**, *58*, 1562–1571.

(4) Lies, D. P.; Hernandez, M. E.; Kappler, A.; Mielke, R. E.; Gralnick, J. A.; Newman, D. K. *Shewanella oneidensis* MR-1 uses overlapping pathways for iron reduction at a distance and by direct contact under conditions relevant for biofilms. *Appl. Environ. Microbiol.* **2005**, *71*, 4414–4426.

(5) Marsili, E.; Baron, D. B.; Shikhare, I. D.; Coursolle, D.; Gralnick, J. A.; Bond, D. R. Shewanella secretes flavins that mediate extracellular electron transfer. *Proc. Natl. Acad. Sci. U.S.A.* **2008**, *105*, 3968–3973.

(6) Rabaey, K.; Boon, N.; Höfte, M.; Verstraete, W. Microbial phenazine production enhances electron transfer in biofuel cells. *Environ. Sci. Technol.* **2005**, *39*, 3401–3408.

(7) Reguera, G.; Nevin, K. P.; Nicoll, J. S.; Covalla, S. F.; Woodard, T. L.; Lovley, D. R. Biofilm and nanowire production leads to increased current in *Geobacter sulfurreducens* fuel cells. *Appl. Environ. Microbiol.* **2006**, *72*, 7345–7348.

(8) Watanabe, K.; Manefield, M.; Lee, M.; Kouzuma, A. Electron shuttles in biotechnology. *Curr. Opin. Biotechnol.* **2009**, *20*, 633–641.

(9) Gorby, Y. A.; Yanina, S.; McLean, J. S.; Rosso, K. M.; Moyles, D.; Dohnalkova, A.; Beveridge, T. J.; Chang, I. S.; Kim, B. H.; Kim, K. S.; Culley, D. E.; Reed, S. B.; Romine, M. F.; Saffarini, D. A.; Hill, E. A.; Shi, L.; Elias, D. A.; Kennedy, D. W.; Pinchuk, G.; Watanabe, K.; Ishii, S.; Logan, B.; Nealson, K. H.; Fredrickson, J. K. Electrically conductive bacterial nanowires produced by *Shewanella oneidensis* strain MR-1 and other microorganisms. *Proc. Natl. Acad. Sci. U.S.A.* **2006**, *103*, 11358–11363.

(10) Logan, B. E.; Regan, J. M. Electricity-producing bacterial communities in microbial fuel cells. *Trends Microbiol.* **2006**, *14*, 512–518.

(11) Rabaey, K.; Rodriguez, J.; Blackall, L. L.; Keller, J.; Gross, P.; Batstone, D.; Verstraete, W.; Nealson, K. H. Microbial ecology meets electrochemistry: Electricity-driven and driving communities. *ISME J.* **2007**, *1*, 9–18.

(12) Girguis, P. R.; Nielsen, M. E.; Figueroa, I. Harnessing energy from marine productivity using bioelectrochemical systems. *Curr. Opin. Biotechnol.* **2010**, *21*, 252–258.

(13) Du, Z.; Li, H.; Gu, T. A state of the art review on microbial fuel cells: A promising technology for wastewater treatment and bioenergy. *Biotechnol. Adv.* **2007**, *25*, 464–482.

(14) Oh, S. T.; Kim, J. R.; Premier, G. C.; Lee, T. H.; Kim, C.; Sloan, W. T. Sustainable wastewater treatment: How might microbial fuel cells contribute? *Biotechnol. Adv.* **2010**, *28*, 871–881.

(15) Feng, Y.; Wang, X.; Logan, B. E.; Lee, H. Brewery wastewater treatment using air-cathode microbial fuel cells. *Appl. Microbiol. Biotechnol.* **2008**, *78*, 873–880.

(16) Rabaey, K.; Bützer, S.; Brown, S.; Keller, J.; Rozendal, R. A. High current generation coupled to caustic production using a lamellar bioelectrochemical system. *Environ. Sci. Technol.* **2010**, *44*, 4315–4321.

(17) Bullen, R. A.; Arnot, T. C.; Lakeman, J. B.; Walsh, F. C. Biofuel cells and their development. *Biosens. Bioelectron.* **2006**, *21*, 2015–2045.

(18) Logan, B. E. Simultaneous wastewater treatment and biological electricity generation. *Water Sci. Technol.* **2005**, *52*, 31–37.

(19) Shukla, A. K.; Suresh, P.; Berchmans, S.; Rajendran, A. Biological fuel cells and their applications. *Curr. Sci.* **2004**, *87*, 455–468.

(20) Tender, L. M.; Gray, S. A.; Groveman, E.; Lowy, D. A.; Kauffman, P.; Melhado, J.; Tyce, R. C.; Flynn, D.; Petrecca, R.; Dobarro, J. The first demonstration of a microbial fuel cell as a viable power supply: Powering a meteorological buoy. *J. Power Sources* **2008**, *179*, 571–575.

(21) Shantaram, A.; Beyenal, H.; Raajan, R.; Veluchamy, A.; Lewandowski, Z. Wireless sensors powered by microbial fuel cells. *Environ. Sci. Technol.* **2005**, *39*, 5037–5042.

(22) Nielsen, M. E.; Reimers, C. E.; Stecher, H. A. Enhanced power from chambered benthic microbial fuel cells. *Environ. Sci. Technol.* **2007**, *41*, 7895–7900.

(23) Rezaei, F.; Richard, T. L.; Brennan, R. A.; Logan, B. E. Substrate-enhanced microbial fuel cells for improved remote power generation from sediment-based systems. *Environ. Sci. Technol.* **2007**, *41*, 4053–4058.

(24) Tender, L. M.; Reimers, C. E.; Stecher, H. A.; Holmes, D. E.; Bond, D. R.; Lowy, D. A.; Pilobello, K.; Fertig, S. J.; Lovley, D. R. Harnessing microbially generated power on the seafloor. *Nat. Biotechnol.* **2002**, *20*, 821–825.

(25) Zuo, Y.; Maness, P.-C.; Logan, B. E. Electricity production from steam-exploded corn stover biomass. *Energy Fuels* **2006**, *20*, 1716–1721.

(26) Reimers, C. E.; Girguis, P.; Stecher, H. A.; Tender, L. M.; Ryckelynck, N.; Whaling, P. Microbial fuel cell energy from an ocean cold seep. *Geobiology* **2006**, *4*, 123–136.

(27) Fan, Y.; Hu, H.; Liu, H. Sustainable power generation in microbial fuel cells using bicarbonate buffer and proton transfer mechanisms. *Environ. Sci. Technol.* **2007**, *41*, 8154–8158.

(28) Liu, H.; Cheng, S.; Huang, L.; Logan, B. E. Scale-up of membrane-free single-chamber microbial fuel cells. *J. Power Sources* **2008**, *179*, 274–279.

(29) Rozendal, R. A.; Hamelers, H. V. M; Rabaey, K.; Keller, J.; Buisman, C. J. N. Towards practical implementation of bioelectrochemical wastewater treatment. *Trends Biotechnol.* **2008**, No. 26, 450–459.

(30) Dewan, A.; Beyenal, H.; Lewandowski, Z. Scaling up microbial fuel cells. *Environ. Sci. Technol.* **2008**, *42*, 7643–7648.

(31) Abrevaya, X. C.; Sacco, N.; Mauas, P. J. D.; Cortón, E. Archaea-based microbial fuel cell operating at high ionic strength conditions. *Extremophiles* **2011**, *15*, 633–642.

(32) Raghavulu, S. V.; Goud, R. K.; Sarma, P. N.; Mohan, S. V. *Saccharomyces cerevisiae* as anodic biocatalyst for power generation in biofuel cell: Influence of redox condition and substrate load. *Bioresour. Technol.* **2011**, *102*, 2751–2757.

(33) Yi, H.; Nevin, K. P.; Kim, B.-C.; Franks, A. E.; Klimes, A.; Tender, L. M.; Lovley, D. R. Selection of a variant of *Geobacter sulfurreducens* with enhanced capacity for current production in microbial fuel cells. *Biosens. Bioelectron.* **2009**, *24*, 3498–3503.

(34) Rabaey, K.; Boon, N.; Siciliano, S. D.; Verhaege, M.; Verstraete, W. Biofuel cells select for microbial consortia that self-mediate electron transfer. *Appl. Environ. Microbiol.* **2004**, *70*, 5373–5382.

(35) Pant, D.; Van Bogaert, G.; Diels, L.; Vanbroekhoven, K. A review of the substrates used in microbial fuel cells (MFCs) for

sustainable energy production. *Bioresour. Technol.* **2010**, *101*, 1533−1543.
(36) Nielsen, M. E.; Wu, D. M.; Girguis, P. R.; Reimers, C. E. Influence of substrate on electron transfer mechanisms in chambered benthic microbial fuel cells. *Environ. Sci. Technol.* **2009**, *43*, 8671−8677.
(37) Catal, T.; Li, K.; Bermek, H.; Liu, H. Electricity production from twelve monosaccharides using microbial fuel cells. *J. Power Sources* **2008**, *175*, 196−200.
(38) Scott, K.; Cotlarciuc, I.; Hall, D.; Lakeman, J. B.; Browning, D. Power from marine sediment fuel cells: The influence of anode material. *J. Appl. Electrochem.* **2008**, *38*, 1313−1319.
(39) Lowy, D. A.; Tender, L. M.; Zeikus, J. G.; Park, D. H.; Lovley, D. R. Harvesting energy from the marine sediment-water interface. II. Kinetic activity of anode materials. *Biosens. Bioelectron.* **2006**, *21*, 2058−2063.
(40) Liu, R.-H.; Sheng, G.-P.; Sun, M.; Zang, G.-L.; Li, W.-W.; Tong, Z.-H.; Dong, F.; Lam, M. H.-W.; Yu, H.-Q.; Hon-Wah Lam, M. Enhanced reductive degradation of methyl orange in a microbial fuel cell through cathode modification with redox mediators. *Appl. Microbiol. Biotechnol.* **2011**, *89*, 201−208.
(41) Milliken, C. E.; May, H. D. Sustained generation of electricity by the spore-forming, Gram-positive, *Desulfitobacterium hafniense* strain DCB2. *Appl. Microbiol. Biotechnol.* **2007**, *73*, 1180−1189.
(42) Torres, C. I.; Marcus, A. K.; Rittmann, B. E.; Legacy, N. Z. Proton transport inside the biofilm limits electrical current generation by anode-respiring bacteria. *Biotechnol. Bioeng.* **2008**, *100*, 872−881.
(43) Rozendal, R. A.; Hamelers, H. V. M; Molenkamp, R. J.; Buisman, C. J. N. Performance of single chamber biocatalyzed electrolysis with different types of ion exchange membranes. *Water Res.* **2007**, *41*, 1984−1994.
(44) Grondin, F.; Perrier, M.; Tartakovsky, B. Microbial fuel cell operation with intermittent connection of the electrical load. *J. Power Sources* **2012**, *208*, 18−23.
(45) Dewan, A.; Beyenal, H.; Lewandowski, Z. Intermittent energy harvesting improves the performance of microbial fuel cells. *Environ. Sci. Technol.* **2009**, *43*, 4600−4605.
(46) Liang, P.; Wu, W.; Wei, J.; Yuan, L.; Xia, X.; Huang, X. Alternate charging and discharging of capacitor to enhance the electron production of bioelectrochemical systems. *Environ. Sci. Technol.* **2011**, *45*, 6647−6653.
(47) White, H. K.; Reimers, C. E.; Cordes, E. E.; Dilly, G. F.; Girguis, P. R. Quantitative population dynamics of microbial communities in plankton-fed microbial fuel cells. *ISME J.* **2009**, *3*, 635−646.
(48) Torres, C. I.; Krajmalnik-Brown, R.; Parameswaran, P.; Marcus, A. K.; Wanger, G.; Gorby, Y. A.; Rittmann, B. E. Selecting anode-respiring bacteria based on anode potential: Phylogenetic, electrochemical, and microscopic characterization. *Environ. Sci. Technol.* **2009**, *43*, 9519−9524.
(49) Lee, H.-S.; Torres, C. I.; Rittmann, B. E. Effects of substrate diffusion and anode potential on kinetic parameters for anode-respiring bacteria. *Environ. Sci. Technol.* **2009**, *43*, 7571−7577.
(50) Nielsen, M. E.; Reimers, C. E.; White, H. K.; Sharma, S.; Girguis, P. R. Sustainable energy from deep ocean cold seeps. *Energy Environ. Sci.* **2008**, *1*, 584−593.
(51) Margulies, M.; Egholm, M.; Altman, W. E.; Attiya, S.; Bader, J. S.; Bemben, L. A.; Berka, J.; Braverman, M. S.; Chen, Y.-J.; Chen, Z.; Dewell, S. B.; Du, L.; Fierro, J. M.; Gomes, X. V.; Godwin, B. C.; He, W.; Helgesen, S.; Ho, C. H.; Irzyk, G. P.; Jando, S. C.; Alenquer, M. L. I.; Jarvie, T. P.; Jirage, K. B.; Kim, J.-B.; Knight, J. R.; Lanza, J. R.; Leamon, J. H.; Lefkowitz, S. M.; Lei, M.; Li, J.; Lohman, K. L.; Lu, H.; Makhijani, V. B.; McDade, K. E.; McKenna, M. P.; Myers, E. W.; Nickerson, E.; Nobile, J. R.; Plant, R.; Puc, B. P.; Ronan, M. T.; Roth, G. T.; Sarkis, G. J.; Simons, J. F.; Simpson, J. W.; Srinivasan, M.; Tartaro, K. R.; Tomasz, A.; Vogt, K. A.; Volkmer, G. A.; Wang, S. H.; Wang, Y.; Weiner, M. P.; Yu, P.; Begley, R. F.; Rothberg, J. M. Genome sequencing in microfabricated high-density picolitre reactors. *Nature* **2005**, *437*, 376−380.
(52) Caporaso, J. G.; Kuczynski, J.; Stombaugh, J.; Bittinger, K.; Bushman, F. D.; Costello, E. K.; Fierer, N.; Peña, A. G.; Goodrich, J. K.; Gordon, J. I.; Huttley, G. A.; Kelley, S. T.; Knights, D.; Koenig, J. E.; Ley, R. E.; Lozupone, C. A.; Mcdonald, D.; Muegge, B. D.; Pirrung, M.; Reeder, J.; Sevinsky, J. R.; Turnbaugh, P. J.; Walters, W. A.; Widmann, J.; Yatsunenko, T.; Zaneveld, J.; Knight, R. QIIME allows analysis of high-throughput community sequencing data intensity normalization improves color calling in SOLiD sequencing. *Nat. Methods* **2010**, *7*, 335−336.
(53) Bard, A. J.; Faulkner, L. R. *Electrochemical Methods: Fundamentals and Applications*, 2nd ed.; John Wiley & Sons, Inc.: New York, 2000; p 35.
(54) Uría, N.; Berbel, X. M.; Sánchez, O.; Muñoz, F. X.; Mas, J. Transient storage of electrical charge in biofilms of *Shewanella oneidensis* MR-1 growing in a microbial fuel cell. *Environ. Sci. Technol.* **2011**, *45*, 10250−10256.
(55) Schrott, G. D.; Bonanni, P. S.; Robuschi, L.; Esteve-Nunez; Abraham Busalmen, J. P. Electrochemical insight into the mechanism of electron transport in biofilms of *Geobacter sulfurreducens*. *Electrochim. Acta* **2011**, *56*, 10791−10795.
(56) He, Z.; Wagner, N.; Minteer, S. D.; Angenent, L. T. An upflow microbial fuel cell with an interior cathode: Assessment of the internal resistance by impedance spectroscopy. *Environ. Sci. Technol.* **2006**, *40*, 5212−5217.
(57) Ramasamy, R. P.; Ren, Z.; Mench, M. M.; Regan, J. M. Impact of initial biofilm growth on the anode impedance of microbial fuel cells. *Biotechnol. Bioeng.* **2008**, *101*, 101−108.
(58) Millero, F. J.; Lee, K.; Roche, M. Distribution of alkalinity in the surface waters of the major oceans. *Mar. Chem.* **1998**, *60*, 111−130.
(59) Franks, A. E.; Nevin, K. P.; Jia, H.; Izallalen, M.; Woodard, T. L.; Lovley, D. R. Novel strategy for three-dimensional real-time imaging of microbial fuel cell communities: Monitoring the inhibitory effects of proton accumulation within the anode biofilm. *Energy Environ. Sci.* **2009**, *2*, 113−119.
(60) Millero, F. J. Thermodynamics of the carbon dioxide system in the oceans. *Science* **1995**, *59*, 661−677.
(61) Lovley, D. R.; Roden, E. E.; Phillips, E. J. Enzymatic iron and uranium reduction by sulfate-reducing bacteria. *Mar. Geol.* **1993**, *113*, 41−53.
(62) Holmes, D. E.; Bond, D. R.; Lovley, D. R. Electron transfer by *Desulfobulbus propionicus* to Fe(III) and graphite electrodes. *Appl. Environ. Microbiol.* **2004**, *70*, 1234−1237.
(63) Lovley, D. R.; Phillips, E. J. Novel processes for anaerobic sulfate production from elemental sulfur by sulfate-reducing bacteria. *Appl. Environ. Microbiol.* **1994**, *60*, 2394−2399.
(64) Holmes, D. E.; Bond, D. R.; O'Neil, R. A.; Reimers, C. E.; Tender, L. R.; Lovley, D. R. Microbial communities associated with electrodes harvesting electricity from a variety of aquatic sediments. *Microb. Ecol.* **2004**, *48*, 178−190.
(65) Finster, K.; Liesack, W.; Thamdrup, B. Elemental sulfur and thiosulfate disproportionation by *Desulfocapsa sulfoexigens* sp. nov., a new anaerobic bacterium isolated from marine surface sediment. *Appl. Environ. Microbiol.* **1998**, *64*, 119−125.
(66) Rabaey, K.; Rozendal, R. A. Microbial electrosynthesis — Revisiting the electrical route for microbial production. *Nat. Rev. Microbiol.* **2010**, *8*, 706−716.